Aust. J. Phys., 1986, **39**, 369–77

Excitation Function for $^{16}O+^{24}Mg$ Elastic Scattering at $\theta_{c.m.} = 90°$

P. V. Drumm,[A,B] *D. F. Hebbard,*[A] *T. R. Ophel,*[A] *J. Nurzynski,*[A] *Y. Kondō,*[C] *B. A. Robson*[C] *and R. Smith*[C,D]

[A] Department of Nuclear Physics, Research School of Physical Sciences, Australian National University, G.P.O. Box 4, Canberra, A.C.T. 2601.
[B] Present address: Science and Engineering Research Council, Daresbury Laboratory, Daresbury, Warrington WA4 4AD, U.K.
[C] Department of Theoretical Physics, Research School of Physical Sciences, Australian National University, G.P.O. Box 4, Canberra, A.C.T. 2601.
[D] Present address: Analytical Studies Branch, Central Studies Establishment, Department of Defence, P.O. Box 105, Campbell, A.C.T. 2601.

Abstract

The $\theta_{c.m.} = 90°$ excitation function for $^{16}O+^{24}Mg$ elastic scattering, which is only sensitive to even partial waves, has been measured for energies $31{\cdot}6 \leqslant E_{c.m.} \leqslant 45{\cdot}2$ MeV in an attempt to resolve an uncertainty in the sign and magnitude of a proposed parity-dependent term in the ^{16}O–^{24}Mg interaction. The data have been analysed by an optical model potential, which includes both a real parity-dependent interaction and an angular momentum-dependent absorptive term. Both the measurements and calculations show some structure but, since this does not correlate with the energies of the even shape resonances in the ^{16}O–^{24}Mg interaction, no conclusion can be drawn concerning the sign and magnitude of the parity dependence of the ^{16}O–^{24}Mg potential.

1. Introduction

Gross structures observed in the excitation functions for the $^{24}Mg(^{16}O, ^{12}C)^{28}Si$ reaction (Paul *et al.* 1978, 1980; Sanders *et al.* 1980; Nurzynski *et al.* 1981) have been assigned spins and parities by analyses of both angular distribution and excitation function data. The angular distributions generally exhibit a highly oscillatory character and resemble the square of a Legendre polynomial, $P_J^2(\cos\theta)$, suggesting a resonating partial wave of order J (Paul *et al.* 1978; Nurzynski *et al.* 1981). The Argonne group (Paul *et al.* 1980; Sanders *et al.* 1980; Sanders *et al.* 1985) analysed the α-transfer excitation functions at 0°, 90° and 180° (c.m.) in terms of Breit–Wigner resonances added to a distorted wave Born approximation (DWBA) background. In this way, they assigned spins and parities $J^\pi = 20^+$, 23^- and 26^+ to structures at $E_{c.m.} = 27{\cdot}6$, $30{\cdot}8$ and $36{\cdot}2$ MeV, respectively. Robson and Smith (1983) interpreted the gross structures observed in the $^{24}Mg(^{16}O, ^{12}C)^{28}Si$ excitation functions at forward angles in terms of parity doublets of shape resonances mainly in the entrance channel ^{16}O–^{24}Mg potential, which contains both a real parity-dependent interaction and an angular momentum-dependent absorptive term. The parity-dependent term produces the staggering of the even and odd parity shape resonances to form the resonance 'doublets', whilst the angular momentum-dependent absorptive term was chosen to be sufficiently transparent to grazing partial waves so that the corresponding shape

0004-9506/86/030369$02.00

resonances are strongly enhanced. The spins and parities of the resonant structures predicted by Robson and Smith (1983) were found to be in good agreement with those deduced in the earlier empirical analyses.

In the empirical analyses referred to above, however, there was often an ambiguity of one unit in the resonance spins, particularly for analyses based upon angular distribution data. Although the α-transfer excitation function data (Sanders *et al.* 1980) at 0°, 90° and 180° (c.m.) cast some light on the situation, the interpretation of such data requires the correlation of structures at forward angles, where the cross section is relatively large, with structures in the 90° (180°) data, where the cross section is three (two) orders of magnitude smaller. The situation is further complicated as the excitation function data at 180° do not exhibit broad structures as observed in the data at 0° but are highly fractionated. Furthermore, Robson and Smith (1983) pointed out that the theoretical interpretation of the resonant structures observed in the α-transfer data is complicated by the possibility of resonant effects in the exit channel. Such uncertainties in the spins of the resonances, in analyses of the type reported by Robson and Smith, result in uncertainties in both the magnitude and sign of the parity-dependent term in the optical potential inferred from the analysis. Thus, it was considered that a measurement of the 90° (c.m.) excitation function for $^{16}O+^{24}Mg$ elastic scattering, which is sensitive to only *even* partial waves, may place additional constraints on the resonance spins and hence constraints on the parity-dependent part of the ^{16}O–^{24}Mg potential.

2. Experiment

Excitation functions for ^{16}O ions scattered from ^{24}Mg were measured by using beams of ^{16}O ions obtained from the 14UD pelletron accelerator at the Australian National University. The scattered ^{16}O ions were detected in an Enge split-pole magnetic spectrometer at 56·3° in the laboratory frame (90° c.m. for elastic scattering) with an angular acceptance of 1° in the reaction plane and with a solid angle of either 0·76 or 1·06 msr. Identification of the 8^+, 7^+ and 6^+ charge states was made with a multi-element gas-filled detector (Ophel and Johnston 1978) which provided measurements of total energy, differential energy loss, position along the focal plane and the angle of entry of each event. Self-supporting targets, of between 20 and 130 $\mu g\,cm^{-2}$, were made from magnesium, isotopically enriched to better than 99·9% in ^{24}Mg. A small amount of tantalum and titanium were introduced during target manufacture. Carbon and oxygen were the other observed contaminants. The targets, which were surrounded by a liquid nitrogen cooled shroud to minimize carbon build-up, were oriented towards the entrance aperture of the magnet to reduce the energy spread of the detected ions scattered from different depths in the target. A solid state detector, positioned at 30° to the beam direction, was used to monitor target thickness and beam current by using the ^{24}Mg and ^{181}Ta in the target. Charge collection was also monitored with a Faraday cup.

Measurements were made of the yield of ^{16}O ions scattered by ^{24}Mg over the beam energy range from 53·0 to 75·5 MeV, for both elastic and inelastic scattering to the 2^+ first excited state at 1·37 MeV. Over this whole energy range, the 7^+ charge state for detected ions was dominant. An energy spectrum of these ions is shown in Fig. 1. Where possible, the individual charge states (8^+, 7^+, 6^+) were measured. These data were used to develop a correction factor for those target runs in which charge state

6^+ did not fully appear on the detector. Charge state 6^+ varied in intensity from about 30% of the total at the lowest beam energy to 10% at the highest.

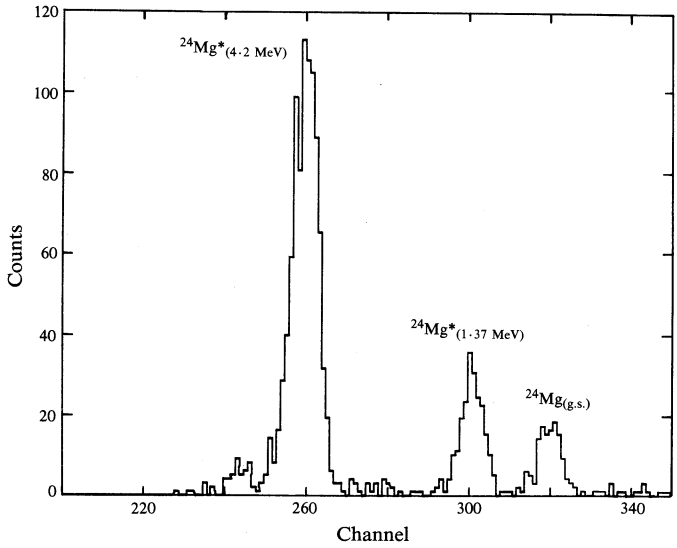

Fig. 1. Energy spectrum of $^{16}O^{7+}$ ions for the scattering of ^{16}O from ^{24}Mg at $E_{lab} = 62$ MeV and $\theta_{c.m.} = 90°$, $\theta_{lab} = 56 \cdot 3°$.

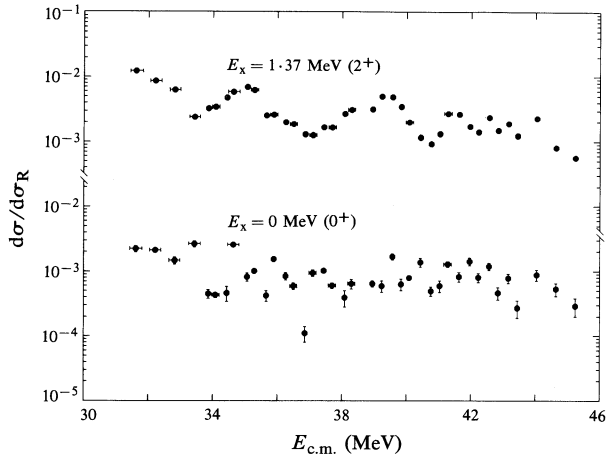

Fig. 2. Excitation functions for inelastic excitation of the 2^+ 1·37 MeV state of ^{24}Mg and for elastic scattering of ^{16}O from ^{24}Mg at 56·3° (lab). The excitation functions are normalized to the Rutherford cross section as discussed in the text.

For the range of energies encompassed by the data from a single target, normalization of the yields to relative cross sections was accomplished either by using the tantalum peak in the 30° monitor detector or by use of the collected charge (corrected for the average charge state of the beam). Both methods gave equivalent results. For

normalizations between different targets, the data on the relative cross sections to the first excited state in ^{24}Mg were adjusted to form a smooth curve. There was sufficient overlap and interleaving of data from different targets for this to be done with assurance. The same adjustment factors were then applied to the elastic scattering data. Finally, absolute normalization of the data, shown in Fig. 2, was achieved by further measurements on two of the targets used above at a beam energy of 37 MeV and at scattering angles of 20° and 30° (lab). At this energy and these angles, there was no evidence for any reaction of ^{16}O on ^{24}Mg other than elastic scattering and approximately 5% of inelastic scattering to the 1·37 MeV state. The elastic scattering cross section at this energy was therefore assumed to be Rutherford. The data were consistent between the monitor detector and the magnetic spectrometer for each target, showing that the charge states of detected ions were properly accounted for. The data were also consistent between the two targets, showing that the relative normalizations developed at the higher energies were consistent.

Errors in the yields of ^{16}O ions were predominantly statistical, scaled if necessary by the charge state correction factor. Error in the determination of this factor, while included, makes no significant contribution. Error in the normalization for the same target at different energies also makes no significant contribution. Normalization between different targets has been assigned an error of $\pm 10\%$, comparable with the statistical error of the inelastically scattered group. These are the sources of the vertical error bars shown in Fig. 2. A further $\pm 20\%$ error (not shown) exists in the absolute normalization. For some targets, clean well-resolved peaks were obtained. However, in many cases, peak statistics were very poor and difficulty was encountered when attempts were made to introduce a reliable background estimate. Finally it was decided to assume that all the data consisted of uncontaminated peaks.

Each data point is plotted at an energy corresponding to the mid-target energy and the range of energies due to target thickness [typically ± 100 keV (c.m.)] is indicated by a horizontal bar. Where a data point shows an average cross section from two or more different targets, the larger target thickness is indicated.

3. Analysis and Results

The measured 90° (c.m.) excitation function for elastic scattering of ^{16}O ions from ^{24}Mg has been analysed in terms of an extended optical model. The ^{16}O–^{24}Mg potential was assumed to have the following form:

$$U(r) = C(r) + (V + \mathrm{i}\,W)g(r), \tag{1}$$

where $C(r)$ is the Coulomb potential for a uniform charge distribution of radius R and $g(r)$ is the Woods–Saxon form factor with diffuseness a and radius

$$R = r_0(A_{\mathrm{proj}}^{1/3} + A_{\mathrm{targ}}^{1/3}). \tag{2}$$

The depth of the real nuclear potential, for orbital angular momentum L, is given by

$$V = V_0 + V_{\mathrm{E}}\, E_{\mathrm{c.m.}} + (-1)^L V_\pi, \tag{3}$$

and consists of three terms, namely a constant V_0, an energy-dependent part and a parity-dependent term. The imaginary part was assumed to be both energy- and

angular momentum-dependent:

$$W = (W_0 + W_E E_{c.m.})[1 + \exp\{(J - J_c)/\Delta\}]^{-1}, \quad (4)$$

where W_0 and W_E are constants, J is the angular momentum, J_c is a cut-off angular momentum and Δ is a diffuseness parameter. The last factor of equation (4) causes the potential to be relatively transparent for partial waves of angular momentum $J \gtrsim J_c$. The energy dependence of J_c was parametrized by the expression (Chatwin *et al.* 1970)

$$J_c = \overline{R}\{(2\mu/\hbar^2)(E_{c.m.} - \overline{Q})\}^{1/2}, \quad (5)$$

in terms of an average radius $\overline{R}$ and an average threshold energy $\overline{Q}$ for the predominant non-elastic reactions. The quantity μ is the reduced mass of the system.

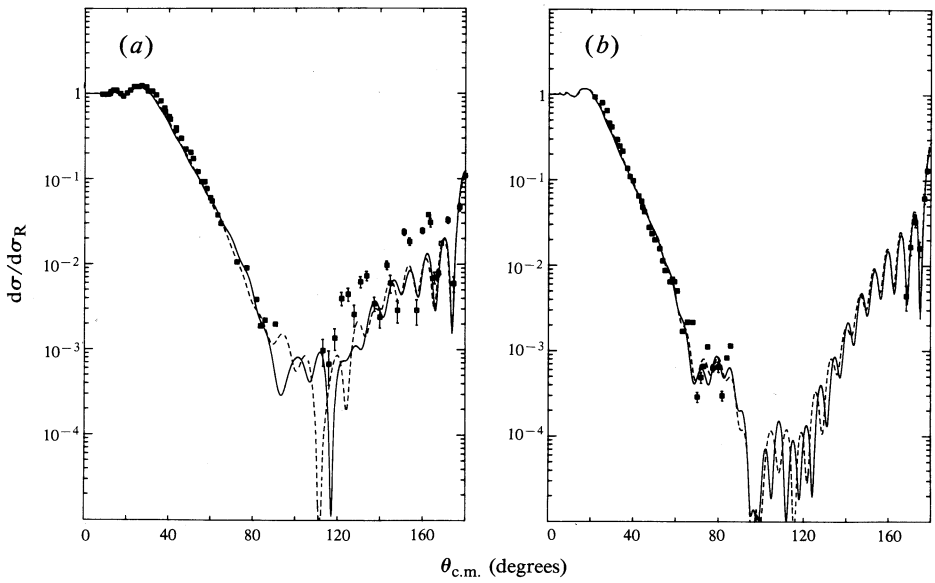

Fig. 3. Angular distributions for elastic scattering of ^{16}O from ^{24}Mg at $E_{c.m.}$ values of (*a*) 27·8 MeV and (*b*) 36·1 MeV. Optical model calculations using potential 1 (solid curves) and potential 2 (dashed curves) are compared with the data of Paul *et al.* (1980) and Siwek-Wilczyńska *et al.* (1974).

The real optical model parameters were obtained in the following way. Firstly, the parameters r_0 and a were chosen. A number of Woods–Saxon geometries were tried and the final values $r_0 = 1{\cdot}35$ fm and $a = 0{\cdot}60$ fm were selected as these gave the best description of the fall-off of the elastic scattering angular distributions (Paul *et al.* 1980; Siwek-Wilczyńska *et al.* 1974) as shown in Fig. 3 at forward angles. Secondly, the parameters V_0, V_E and V_π were obtained by requiring that the real potential gives shape resonances (i.e. partial waves with nuclear phases of $\frac{1}{2}\pi$) with spins 20, 23 and 26 at $E_{c.m.}$ values of 27·6, 30·8 and 36·2 MeV, respectively, in agreement with those determined empirically (Paul *et al.* 1980). In accord with the analysis

of Robson and Smith (1983), these shape resonances were assumed to be the lowest energy (zero node) states of the appropriate angular momenta. The derived values of the parameters are shown in Table 1 as potential 1. A second set (potential 2) was determined in a similar manner assuming that the spin of each resonance was one unit smaller, i.e. 19, 22 and 25, respectively, as allowed by assigning an uncertainty of one unit to the resonance spins determined by Paul *et al.* (1978) and Nurzynski *et al.* (1981). It should be noted that the main effect upon the real optical model parameters of this one unit shift in the resonance spins is that potentials 1 and 2 have opposite signs for the parity-dependent term V_{π}.

Table 1. Optical model potentials

For all potentials $r_0 = 1{\cdot}35$ fm, $a = 0{\cdot}60$ fm and $\Delta = 0{\cdot}80$

No.	V_0 (MeV)	V_E	V_{π} (MeV)	W_0 (MeV)	W_E	$\overline{R}$ (fm)	$\overline{Q}$ (MeV)
1	−1·51	−0·71	1·20	11·33	−0·89	10·63	17·34
2	−1·39	−0·59	−1·07	9·47	−0·75	9·88	14·51
3	−1·51	−0·71	1·20	11·33	−0·89	8·32	16·45
4	−1·39	−0·59	−1·07	9·47	−0·75	8·13	17·13

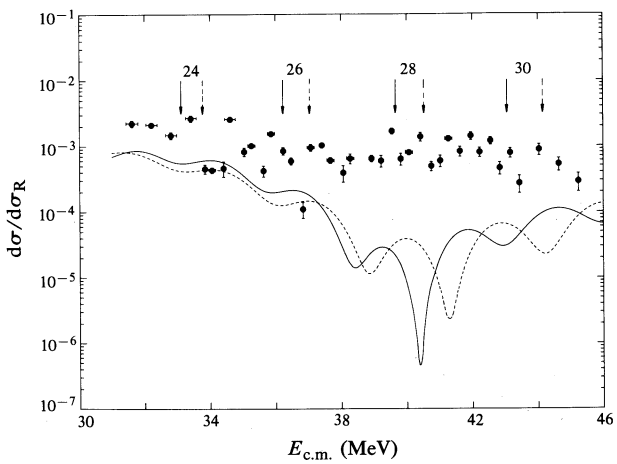

Fig. 4. Excitation function for elastic scattering of ^{16}O from ^{24}Mg at $\theta_{c.m.} = 90°$. The solid and dashed curves are optical model calculations for potentials 1 and 2, respectively. The solid and dashed arrows denote the resonance energies of the corresponding even angular momentum shape resonances.

The parameters of the absorptive potential were then determined by least-squares fitting of angular distributions at 27·8 and 36·1 MeV for which both forward and backward angle data are available (Paul *et al.* 1980; Siwek-Wilczyńska *et al.* 1974). The latter angular distribution comprises forward angle data at 36·0 MeV and backward angle data at 36·2 MeV. The fits obtained are shown in Fig. 3, where the solid and dashed curves correspond to potentials 1 and 2, respectively. It is seen that both potentials give similar results. From these fits, values of W_0, W_E, $\overline{R}$ and $\overline{Q}$ were determined and are given in Table 1. A value $\Delta = 0{\cdot}8$, which was employed previously (Robson and Smith 1983), was used throughout the present work.

In Fig. 4 calculated elastic excitation functions at $\theta_{c.m.} = 90°$ for both potential 1 (solid curve) and potential 2 (dashed curve) are compared with the measured excitation function. It is seen that neither potential provides a satisfactory description of the data. Therefore it is not possible to draw any conclusion about the two alternative potentials and hence any definite conclusion concerning the sign of the parity-dependent term.

A further problem is highlighted by comparison of the results shown in Fig. 4 with the energies at which the even spin shape resonances for both potentials 1 and 2 occur. These resonance energies, which were chosen to match assigned resonances in the $^{24}Mg(^{16}O, ^{12}C)^{28}Si$ reaction data, are denoted by a set of arrows for each potential. As can be seen, for the energy range $31{\cdot}6 \leqslant E_{c.m.} \leqslant 45{\cdot}2$ MeV, both potentials predict four even spin resonances. Obviously, neither of the predictions shown in Fig. 4 (nor the experimental data) exhibit any apparent correlation with these energies. The reason for this lack of correlation is that the potentials are not sufficiently transparent to the resonating partial waves for the underlying shape resonances to produce any discernible effects in the calculated excitation functions.

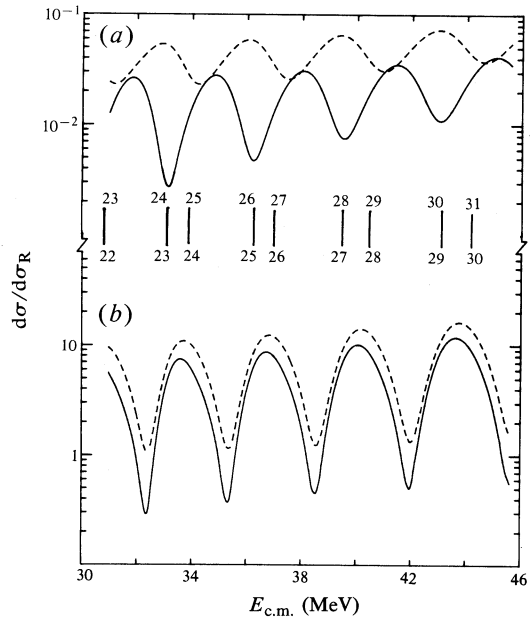

Fig. 5. Optical model calculations for elastic scattering of ^{16}O from ^{24}Mg at $\theta_{c.m.}$ values of (*a*) 90° and (*b*) 180°. The solid and dashed curves are the predictions for potentials 3 and 4, respectively. The short vertical lines in the centre denote the resonance energies and the upper and lower numbers indicate the corresponding spins of the resonating partial waves for potentials 3 and 4, respectively.

In order to demonstrate the kind of effects which can arise from the resonating partial waves, in a more favourable situation in which the optical potential is more transparent, we have modified potentials 1 and 2 accordingly. The solid curves of Fig. 5 are the predicted 90° and 180° excitation functions for potential 3 of Table 1. This potential corresponds to the case in which potential 1 has been made more

transparent by adjusting the values of $\overline{R}$ and $\overline{Q}$ so that J_c is approximately one unit less than the spins of the even partial waves at their resonance energies. The dashed curves show the corresponding results for a more transparent form of potential 2 (No. 4 of Table 1). In this case, the values of J_c are about one unit less than the spins of the odd partial waves at their resonance energies. It is seen that, in both cases, the 180° excitation functions (*b*) display maxima near the doublets of resonance energies indicated by short vertical lines in the centre (the numbers above and below the lines are the spins of the resonating partial waves for potentials 3 and 4, respectively) so that the two curves are *in phase*. On the other hand, the corresponding 90° excitation functions (*a*) are essentially *out of phase* with one another. This indicates that a measurement of the 90° excitation function should allow one to distinguish between two sets of spin assignments differing by one unit provided the optical potential is sufficiently transparent to the resonating partial waves.

4. Conclusions

The $\theta_{c.m.} = 90°$ excitation function has been measured for energies $31{\cdot}6 \leqslant E_{c.m.} \leqslant 45{\cdot}2$ MeV. The data have been described in terms of an optical model potential, which contains both a real parity-dependent interaction and an angular momentum-dependent absorptive term. Two sets of optical model parameters, based upon spin assignments to gross structures observed in the $^{24}Mg(^{16}O, ^{12}C)^{28}Si$ reaction and fits to elastic scattering angular distributions, have been used. The main difference between the two sets is that they have opposite signs for the parity-dependent term resulting from a difference of one unit in the spins of the resonating partial waves. Since neither parameter set gives a satisfactory description of the data, it is not possible to draw any definite conclusion concerning the sign of the parity-dependent term in the ^{16}O–^{24}Mg interaction. This ambiguity arises because both potentials absorb the resonating partial waves too strongly so that their resonance effects are masked by diffraction phenomena. Corresponding potentials, which are sufficiently more transparent to the resonating partial waves, predict $\theta_{c.m.} = 90°$ excitation functions which are out of phase with one another and so allow one to distinguish the sign of the parity-dependent term. One system for which this situation may occur is $^{16}O+^{20}Ne$ (Schimizu *et al.* 1983, 1986) for which the elastic scattering at backward angles is not only considerably larger than for $^{16}O+^{24}Mg$ elastic scattering but also exhibits gross structures as a function of energy, unlike $^{16}O+^{24}Mg$.

References

Chatwin, R. A., Eck, J. S., Robson, D., and Richter, A. (1970). *Phys. Rev.* C **1**, 795.

Nurzynski, J., Ophel, T. R., Clark, P. D., Eck, J. S., Hebbard, D. F., Weisser, D. C., Robson, B. A., and Smith R. (1981). *Nucl. Phys.* A **363**, 253.

Ophel, T. R., and Johnston, A. (1978). *Nucl. Instrum. Methods* **157**, 461.

Paul, M., Sanders, S. J., Cseh, J., Geesaman, D. F., Henning, W., Kovar, D. G., Olmer, C., and Schiffer, J. P. (1978). *Phys. Rev. Lett.* **40**, 1310.

Paul, M., Sanders, S. J., Geesaman, D. F., Henning, W., Kovar, D. G., Olmer, C., and Schiffer, J. P. (1980). *Phys. Rev.* C **21**, 1802.

Robson, B. A., and Smith, R. (1983). *Phys. Lett.* B **123**, 160.

Sanders, S. J., Ernst, H., Henning, W., Jachcinski, C., Kovar, D. G., Schiffer, J. P., and Barrette, J. (1985). *Phys. Rev.* C **31**, 1775.

Sanders, S. J., Paul, M., Cseh, J., Geesaman, D. F., Henning, W., Kovar, D. G., Kozub, R., Olmer, C., and Schiffer, J. P. (1980). *Phys. Rev.* C **21**, 1810.

Schimizu, J., Nagashima, Y., Nakagawa, T., Fukuchi, Y., Yokota, W., Furuno, K., and Kubono, S. (1986). Resonances in the $^{16}O+^{20}Ne$ reactions from $E_{c.m.} = 23$ to 38 MeV. (To be published).

Schimizu, J., Yokota, W., Nakagawa, T., Fukuchi, Y., Yamaguchi, H., Sato, M., Hanashima, S., Nagashima, Y., Furuno, K., Katori, K., and Kubono, S. (1983). *Phys. Lett.* B **112**, 323.

Siwek-Wilczyńska, K., Wilczyński, J., and Christensen, P. R. (1974). *Nucl. Phys.* A **229**, 461.

Manuscript received 22 November 1985, accepted 28 February 1986